Table IV. Dipole Moments (D) of Phosphine–Borane Derivatives

$(CH_3)_3P\cdot BH_3$	4.99 ± 0.02[a]	$F_3P\cdot BH_3$	1.64 ± 0.02[c]
$(CH_3)_2PH\cdot BH_3$	4.85 ± 0.06[b]	$F_2HP\cdot BH_3$	2.50 ± 0.03[d]
$CH_3PH_2\cdot BH_3$	4.66 ± 0.05[a]	$H_3P\cdot BH_3$	4.00 ± 0.03[e]
		$H_3P\cdot BF_3$	3.73 ± 0.3[f]

[a] Reference 12. [b] Reference 15. [c] Reference 14. [d] Reference 13. [e] Reference 11. [f] This work.

terium exchange was a problem as well. Typical spectra showed strong lines attributable to the mixed H–D species of phosphine. These were 10–20 times stronger than $H_3P\cdot BF_3$ lines (depending upon pressures from 90 to 33 mTorr).

Inductive effects of substituents in relation to dipole moments in phosphine–boranes might predict the dipole moment in $H_3P\cdot BF_3$ to be higher than in $H_3P\cdot BH_3$. In Table IV it is shown that an inductive effect is qualitatively consistent when substitution is on the phosphorus atom. Simplified σ inductive effects then are not sufficient to rationalize the value of the dipole moment in $H_3P\cdot BF_3$. Additionally, since the dipole moment of $H_3P\cdot BCl_3$ in benzene solution has been found[15] to be 5.2 ± 0.1 D, we expected the moment in $H_3P\cdot BF_3$ in the gas phase to be of comparable magnitude. At this time we are unable to explain this apparent discrepancy. It would be interesting to compare the dipole moments in some $R_3N–BF_3$ compounds with those in corresponding $-BCl_3$ and $-BH_3$ analogs.

The barrier in $H_3P\cdot BF_3$ is larger than in $H_3P\cdot BH_3$. Fink and Allen[28] have proposed a model for explaining barrier trends which offers a balance of the sum of a nuclear–electronic potential (V_{ne}), a nuclear–nuclear potential (V_{nn}), and a kinetic term (T) with the electron–electron repulsive potential (V_{ee}) as the factor determining the barriers. This model has been used qualitatively for other coordination compounds of phosphorus and boron.[1,7] Ab initio calculations[29] on $H_3P\cdot BH_3$ have shown that the inclusion of phosphorus d-orbital overlap raises the calculated barrier and it approaches the experimental value.

This d-orbital overlap must involve hyperconjugation in the BH_3 moiety. Since the likelihood of this effect is absent in $H_3P\cdot BF_3$, we must consider the sum of the contributions of the individual terms of Allen's theory. Fluorine substitution, because of the greater atomic charge and large number of electrons, might be expected to increase the barrier through the V_{nn} and V_{ee} terms, while the V_{ne} term might lower the barrier. Qualitatively, these effects can explain both a higher barrier in $H_3P\cdot BF_3$ than in $H_3P\cdot BH_3$ and the fact that the barriers in $H_3P\cdot BF_3$ and $F_3P\cdot BH_3$ are similar.

Acknowledgment. The authors gratefully acknowledge the financial support of this work by the National Science Foundation through Grant GP-42907X.

Registry No. $H_3P\cdot{}^{11}BF_3$, 56298-59-0; $D_3P\cdot{}^{11}BF_3$, 56272-33-4; $H_3P\cdot{}^{10}BF_3$, 56272-34-5; $D_3P\cdot{}^{10}BF_3$, 56510-53-3.

References and Notes

(1) Part X: J. R. Durig, B. A. Hudgens, Y. S. Li, and J. D. Odom, *J. Chem. Phys.*, **61**, 4890 (1974).
(2) Taken in part from the thesis of V. F. Kalasinsky, submitted to the Department of Chemistry in partial fulfillment of the Ph.D. degree, May 1975.
(3) J. R. Durig, Y. S. Li, L. A. Carreira, and J. D. Odom, *J. Am. Chem. Soc.*, **95**, 2491 (1973).
(4) P. S. Bryan and R. L. Kuczkowski, *Inorg. Chem.*, **11**, 553 (1972).
(5) R. L. Kuczkowski and D. R. Lide, Jr., *J. Chem. Phys.*, **46**, 357 (1967).
(6) J. P. Pasinski and R. L. Kuczkowski, *J. Chem. Phys.*, **54**, 1903 (1971).
(7) J. R. Durig, V. F. Kalasinsky, Y. S. Li, and J. D. Odom, *J. Phys. Chem.*, **79**, 468 (1975).
(8) J. D. Odom, V. F. Kalasinsky, and J. R. Durig, *J. Mol. Struct.*, **24**, 139 (1975).
(9) J. R. Durig, S. Riethmiller, V. F. Kalasinsky, and J. D. Odom, *Inorg. Chem.*, **13**, 2729 (1974).
(10) J. E. Drake, J. L. Hencher, and B. Rapp, *J. Chem. Soc., Dalton Trans.*, 595 (1974).
(11) J. D. Odom, S. Riethmiller, S. J. Meischen, and J. R. Durig, *J. Mol. Struct.*, **20**, 471 (1974).
(12) J. D. Odom, B. A. Hudgens, and J. R. Durig, *J. Phys. Chem.*, **77**, 1972 (1973).
(13) J. D. Odom, S. Riethmiller, J. D. Witt, and J. R. Durig, *Inorg. Chem.*, **12**, 1123 (1973).
(14) E. B. Wilson, J. C. Decius, and P. C. Cross, "Molecular Vibrations", McGraw-Hill, New York, N.Y., 1955.
(15) P. A. Tierney, D. W. Lewis, and D. Berg, *J. Inorg. Nucl. Chem.*, **24**, 1163 (1962).
(16) J. D. Odom, V. F. Kalasinsky, and J. R. Durig, *Inorg. Chem.*, **14**, 434 (1975).
(17) D. F. Shriver, "The Manipulation of Air-Sensitive Compounds", McGraw-Hill, New York, N.Y., 1969.
(18) R. C. Marriott, J. D. Odom, and C. T. Sears, *Inorg. Synth.*, **14**, 1 (1973).
(19) J. Dobson and R. Schaeffer, *Inorg. Chem.*, **9**, 2183 (1970).
(20) D. R. Martin and R. E. Dial, *J. Am. Chem. Soc.*, **72**, 852 (1950).
(21) E. Wiberg and U. Heubaum, *Z. Anorg. Allg. Chem.*, **225**, 270 (1935).
(22) J. S. Muenter, *J. Chem. Phys.*, **48**, 4544 (1968).
(23) C. H. Townes and A. L. Schawlow, "Microwave Spectroscopy", McGraw-Hill, New York, N.Y., 1955, p 250.
(24) R. W. Rudolph and R. W. Parry, *J. Am. Chem. Soc.*, **89**, 1621 (1967).
(25) T. D. Coyle and F. G. A. Stone, *Prog. Boron Chem.*, **1**, 137 (1964).
(26) S. Geller and J. L. Hoard, *Acta Crystallogr.*, **3**, 121 (1950); **4**, 399 (1951).
(27) J. L. Hoard, S. Geller, and W. M. Cashin, *Acta Crystallogr.*, **4**, 396 (1951).
(28) W. H. Fink and L. C. Allen, *J. Chem. Phys.*, **46**, 2261 (1967).
(29) J. R. Sabin, *Chem. Phys. Lett.*, **20**, 212 (1973).

Contribution from the Department of Chemistry,
University of South Carolina, Columbia, South Carolina 29208

Spectra and Structure of Some Silicon-Containing Compounds. VIII.[1] Vibrational Spectra of Hexafluorodisiloxane

J. R. DURIG,* V. F. KALASINSKY, and M. J. FLANAGAN[2]

Received March 3, 1975

AIC50154H

The Raman spectra (50–2000 cm^{-1}) of gaseous, liquid, and solid $(F_3Si)_2O$ have been recorded. The infrared spectra of the gas and solid have been recorded from 55 to 2500 cm^{-1}. The spectra of all three physical states have been interpreted in detail on the basis of C_{2v} symmetry. The A_1 skeletal Si–O–Si bend was assigned at 85 cm^{-1} in the infrared spectra. Normal-coordinate calculations using a valence force field gave the Si–O and Si–F stretching force constants as 5.48 ± 0.13 and 5.07 ± 0.08 mdyn/Å, respectively. Extensive mixing was found in the A_1 block, the reasons for which are discussed. Comparisons are made between $(F_3Si)_2O$ and other substituted disiloxanes.

Introduction

Almenningen et al.[3] have found the Si–O–Si angle in disiloxane, $(H_3Si)_2O$, to be 144 ± 1° from electron diffraction investigations of this molecule. Since the skeletal bending mode is found[4] at 68 cm^{-1}, the angle in disiloxane must be increased by an uncertain amount depending on the nature of the potential function governing this bending motion to allow[5,6] for the "shrinkage". The large skeletal angle in disiloxane compared to the corresponding one (112°) in dimethyl ether[7] can be interpreted in terms of the delocalization of the electrons in the lone pairs on the oxygen atom into the vacant 3d silicon orbitals. The replacement of the hydrogen atoms in disiloxane by fluorine atoms, which are highly electron withdrawing, could be expected to enhance this effect. Thus, the skeletal angle is expected to be even larger in hexafluorodisiloxane, $(F_3Si)_2O$, with a shorter Si–O bond than the corresponding quantities in disiloxane which is exactly what was found in a recent electron diffraction study[8] of hexafluorodisiloxane. An Si–O–Si angle of 156 ± 2° and an Si–O distance of 1.580 ± 0.025 Å were reported for $(F_3Si)_2O$ by Airey et al.;[8] they stated that the possibility that the molecule has a potential energy minimum corresponding to a linear Si–O–Si skeleton could not be ruled out. The Si–O distance in disiloxane was reported[3] to be 1.634 ± 0.002 Å. Thus, these results are consistent with an increase in the p_π–d_π bonding in the perfluorodisiloxane molecule. However, Airey et al.[9] reported an Si–O–Si angle of 146° for the hexachlorodisiloxane molecule, although one would expect the skeletal angle in this molecule to be very similar to the one in hexafluorodisiloxane.

We[10] have investigated the infrared spectra of gaseous and solid and the Raman spectra of gaseous, liquid, and solid $(Cl_3Si)_2O$. The spectra of the gas were interpreted on the basis of C_{2v} symmetry but the spectra of the solid gave evidence that there are structural changes upon condensation and that the Si–O–Si angle approaches linearity in the solid state. As a continuation of our studies of silicon-containing compounds we have investigated the Raman spectra of gaseous, liquid, and solid $(F_3Si)_2O$ and the infrared spectra of the gas and solid in order to determine the molecular symmetry of this compound in all three physical states.

There has been little spectroscopic work on hexafluorodisiloxane. Margrave et al.[11] reported that the hydrolysis of SiF_4 yields hexafluorodisiloxane as the major product, and they reported several infrared bands between 672 and 1268 cm^{-1} as being characteristic of the molecule. Hamada and Morishita[12] reported a vibrational–rotational analysis of this molecule and concluded from the fine structure of the two bands at 1186 and 1284 cm^{-1} that the molecule is linear in the gas phase. However, neither of these bands was observed in our infrared study. Therefore, a complete vibrational study has been undertaken and the results are reported herein.

Experimental Section

Hexafluorodisiloxane was prepared by Dr. F. E. Brinckman by the reaction of hexachlorodisiloxane with antimony trifluoride using a trace of antimony pentachloride as a catalyst.[13] The sample was stored prior to use in capillaries designed to withstand high internal pressures. Raman spectra of the liquid taken before and after a 2-year interval did not indicate any sample decomposition.

Margrave et al.[11] have indicated that condensation and subsequent revaporization of hexafluorodisiloxane result in partial decomposition to silicon tetrafluoride and a white polymer. Therefore, it is not at all unreasonable that all attempts to purify this compound were unsuccessful in eliminating silicon tetrafluoride from our sample. In one such attempt, SiF_4 was isolated so that infrared and Raman spectra of the gas could be taken for comparison with the spectra of hexafluorodisiloxane. In this way bands attributable to this impurity could be easily identified.

The Raman spectra were recorded on a Cary Model 82 spectrophotometer equipped with a CRL Model 53G argon ion laser. The 5145-Å exciting line was used throughout, and the power was estimated to be ~1.5 W at the sample. The spectrum of the gas was obtained with the sample contained in a standard Cary multipass cell utilizing a greaseless stopcock. The spectra of the liquid and solid were taken at −45 and −120, respectively, in a sealed capillary. The low-temperature cell used has been previously described by Miller and Harney.[14] Typical spectra are shown in Figure 1.

The mid-infrared spectra were recorded on a Perkin-Elmer Model 621 spectrophotometer. The instrument was purged with dry nitrogen and calibrated in the usual manner.[15] The spectra of the gas were taken at various sample pressures (1–10 mmHg) in a 25-cm glass cell equipped with CsI windows. The spectrum of the annealed solid was obtained with the sample deposited on a CsI plate held at liquid nitrogen temperature in a cold cell similar to one previously described.[16] Mid-infrared spectra are shown in Figure 2.

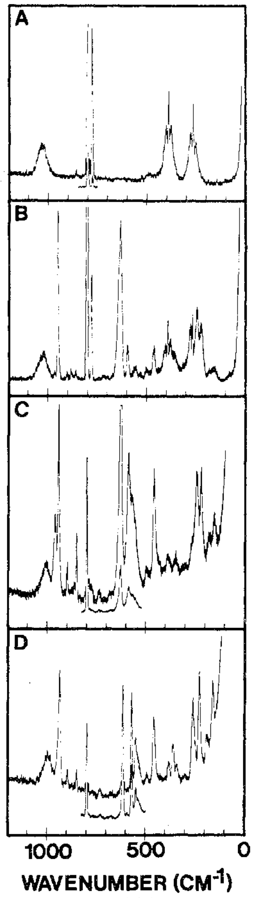

Figure 1. Raman spectra of hexafluorodisiloxane and silicon tetrafluoride: (A) gaseous SiF_4 (room temperature, SBW = 5 cm^{-1}); (B) gaseous Si_2OF_6 (room temperature, SBW = 5 cm^{-1}); (C) liquid Si_2OF_6 (room temperature under pressure, SBW = 4 cm^{-1}); (D) solid Si_2OF_6 (−110°, SBW = 5 cm^{-1}).

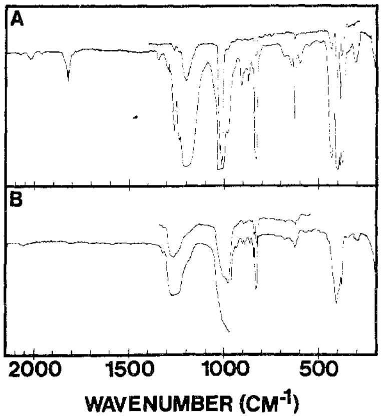

Figure 2. Mid-infrared spectra of hexafluorodisiloxane: (A) gas; (B) solid.

A Beckman Model IR-11 spectrophotometer was employed in taking the far-infrared spectra. The instrument was continuously flushed with dry nitrogen, except during calibration.[17] The spectrum of the gas was taken with the sample (~10 mmHg) contained in a 10 cm Monel cell equipped with polyethylene windows. The spectrum of the solid was recorded utilizing a cold cell similar to one previously described.[16] Modifications include a wedged silicon plate substrate and a liquid nitrogen flow system for improved temperature equilibration. Standard deposition and annealing techniques were used. Portions of the far-infrared spectra of the gas and solid are shown in Figure 3. All frequencies, except those corresponding to very broad

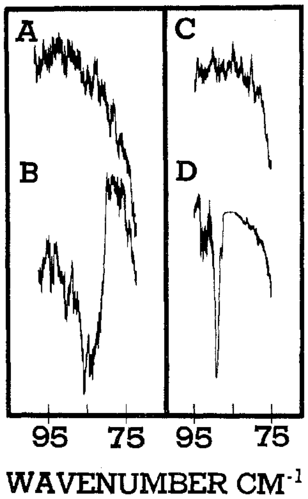

Figure 3. Si–O–Si bending fundamental (ν_7) in the far-infrared spectra of hexafluorodisiloxane: (A) background of the cell; (B) spectrum of the gas; (C) background of the cell; (D) spectrum of the solid.

bands, are expected to be accurate to ±2 cm^{-1}.

Vibrational Assignments

Interpretation of the spectra of hexafluorodisiloxane was complicated by the presence of SiF_4 impurity in our sample. Particularly in the low-frequency region of the Raman spectrum of the gas, SiF_4 modes obscured rather large regions of the spectrum due to their intensity and associated fine structure. The Raman spectrum of gaseous SiF_4 (Figure 1A) clearly shows the four fundamentals for this molecule of T_d symmetry: ν_1, 800 cm^{-1}; ν_2, 264 cm^{-1}; ν_3, 1030 cm^{-1}; ν_4, 388 cm^{-1}.[18] In addition, the infrared spectra are complicated by intense SiF_4 bands centered at 390 and 1026 cm^{-1}. The polarized Raman line at 776 cm^{-1} was at first thought to be the $v = 2 \leftarrow 1$ "hot band" of ν_1. However, the absence of a second "hot band" at high sensitivity led us to believe this frequency to be the overtone $2\nu_4 = 776$ cm^{-1} in Fermi resonance with ν_1 to explain its intensity. A comparison of the spectra given in Figure 1 should make it obvious in most cases which lines in the Raman effect can be attributed to SiF_4.[19]

Several molecular symmetries must be considered in the case of hexafluorodisiloxane which has nine atoms with 21 normal vibrations. The number of infrared- and Raman-active fundamentals differs markedly depending on whether or not the Si–O–Si skeleton is linear or bent. For a bent skeleton, the symmetry may be C_{2v}, if the SiF_3 groups are eclipsed, or C_2, if the SiF_3 groups are twisted. The C_{2v} symmetry spans the irreducible representation $7\ A_1 + 4\ A_2 + 6\ B_1 + 4\ B_2$. The A_2 motions are Raman active only while all others are active in both the infrared and Raman effect. Therefore, all 21 fundamental vibrations should be observed in the Raman spectrum and 17 in the infrared spectrum. The irreducible representation for C_2 symmetry, on the other hand, is $11\ A + 10\ B$ with all 21 fundamental motions active in both the infrared and Raman effects.

The possible symmetries to consider for a linear Si–O–Si skeleton are D_{3h}, D_{3d}, and D_3 depending on the orientation of the SiF_3 groups. For D_{3h} molecular symmetry, the normal vibrations span the irreducible representation $3\ A_1'(R) + A_2'(\text{inactive}) + 3\ A_2''(\text{ir}) + 4E'(R, \text{ir}) + 3E''(R)$ where the activity of the motions in each symmetry block is indicated in parentheses. Thus, 10 modes are Raman active, and 7 motions are infrared active with 4 possible coincidences. For the D_{3d} symmetry, the normal vibrations are represented by $3\ A_{1g}(R) + A_{1u}(\text{inactive}) + 3\ A_{2u}(\text{ir}) + 3E_g(R) + 4\ E_u(\text{ir})$, resulting in 6 Raman-active and 7 infrared-active fundamentals. The center of symmetry for this possible structure dictates mutual exclusion with no infrared and Raman coincidences. The irreducible representations and activity for the D_3 molecular symmetry are $4\ A_1(R) + 3\ A_2(R, \text{ir}) + 7\ E(R, \text{ir})$. Fourteen fundamentals are expected in the Raman effect and 10 in the infrared effect with 10 coincidences. A strictly linear Si–O–Si skeleton need not be present for any one of these three latter symmetries to be applicable. The presence of a very low frequency and highly anharmonic skeletal bending motion may result in a quasilinear molecular structure that is not strictly linear in the ground vibrational state but which still obeys the higher symmetry selection rules. The theory of the quasilinear molecule has been presented by Thorson and Nakagawa.[20]

The infrared and Raman spectra of gaseous hexafluorodisiloxane appear too complicated to be assigned on the basis of a linear or quasilinear Si–O–Si skeleton. The number of observed bands cannot adequately be reduced by assigning combinations or overtones particularly in the Raman effect in which binary combinations, if observed, are expected to be very weak since their observation depends on the electrical and mechanical anharmonicity. The number of infrared and Raman coincidences is less than expected for C_2 or C_{2v} symmetry, presumably because of lack of intensity for some transitions and the presence of SiF_4 impurity obscuring portions of the spectra. The spectra of the liquid and solid do not exhibit distinct changes in band intensities or number of observed bands as was observed in hexachlorodisiloxane.[10] Consequently, the spectra of hexafluorodisiloxane have been interpreted in terms of C_{2v} symmetry for all three physical states. The alternative molecular symmetry is C_2 as previously discussed. However, this symmetry for hexafluorodisiloxane dictates four more infrared and Raman coincidences and an increase of four in the number of polarized Raman fundamentals compared to C_{2v}. For the most part, only the frequencies of the gas are discussed in detail while the Raman frequencies of the liquid and solid and the infrared frequencies of the solid with their accompanying assignments can be found in Table I.

The A_1 SiF_3 symmetric stretch (in-phase) is assigned to the strong, polarized Raman line at 634 cm^{-1} and medium strong infrared counterpart at 631 cm^{-1}. The corresponding out-of-phase motion was observed at 838 cm^{-1} in the infrared spectra. These assignments were made based on the relative intensities of these lines in the infrared and Raman effects as well as their relative positions with respect to the symmetric stretching motion at 800 cm^{-1} in SiF_4.[18]

The SiF_3 antisymmetric stretching motions (in phase) are assigned as accidentally degenerate at 949 cm^{-1} in the Raman effect. The out-of-phase antisymmetric stretches were assigned, also accidentally degenerate, to the strong infrared band at 989 cm^{-1} that appears as a shoulder on the SiF_4 fundamental in that region. In each case the counterpart of the observed frequency was not discernible, presumably due to the lack of intensity and the presence of the strong, broad SiF_4 fundamental obscuring any weak bands. These assignments are consistent with those of other substituted disiloxanes.[10,21] Although the Raman counterpart of the 989-cm^{-1} infrared band was not observed, this frequency was used to assign the A_2 SiF_3 antisymmetric stretching fundamental for the reason given above.

The SiF_3 symmetric deformation in the A_1 block was observed at 557 cm^{-1} in the Raman effect and 555 cm^{-1} in the infrared effect with the corresponding B_1 motion assigned to the infrared band at 402 cm^{-1} coincident with the R branch of the SiF_4 fundamental in that region. The infrared spectrum of the gas (Figure 2A) reveals that ν_4 of SiF_4 is markedly unsymmetrical, suggesting the presence of a band coincident with the fine structure at higher frequency than the band

Table I. Assignment of the Fundamental Vibrations of Hexafluorodisiloxane and PED for the Gas Phase[a]

Species	Solid		Liquid	Gas			
	Raman	Infrared	Raman	Raman	Infrared	Calcd	Assignment and PED for gas
A_1 (R, ir)	934 ms	940 w, sh	942 ms (p)	949 s (p)		957	ν_1 SiF_3 antisym str (87%), SiF_3 antisym def (8%), SiF_3 rock (2%), Si–O–Si bend (3%)
	616 s	628 m, br	630 s (p)	634 s (p)	631 ms	632	ν_2 SiF_3 sym str (100%)
	569 m		588 m (p)	598 mw (p)	601 w	596	ν_3 Si–O–Si sym str (62%), SiF_3 sym def (30%), SiF_3 sym str (8%)
	549 mw	554 vw	571 mw, sh (p)	557 w, br (p)	555 vw br	522	ν_4 SiF_3 sym def (33%), SiF_3 antisym def (21%), Si–O–Si bend (22%), SiF_3 rock (13%), SiF_3 antisym str (11%)
	455 m	453 vw, sh	459 m (p)	461 mw (p)		420	ν_5 SiF_3 antisym def (77%), SiF_3 sym def (11%), Si–O–Si bend (5%), SiF_3 rock (4%), SiF_3 antisym str (3%)
	257 m		244 m (p)	242 m (p)		212	ν_6 SiF_3 rock (32%), SiF_3 sym def (28%), Si–O–Si bend (19%), SiF_3 antisym str (15%), SiF_3 antisym def (6%)
		88 w			85 w	85	ν_7 Si–O–Si bend (53%), SiF_3 rock (34%), SiF_3 sym def (13%)
A_2 (R)	(981)[b]			(989)[b]		993	ν_8 SiF_3 antisym str (92%), SiF_3 antisym def (6%), SiF_3 rock (2%)
	356 mw		354 vw (dp)	358 w (dp)		355	ν_9 SiF_3 antisym def (85%), SiF_3 antisym str (15%)
	155 m		155 w (dp)	157 w (dp)		167	ν_{10} SiF_3 rock (98%), SiF_3 antisym def (2%)
							ν_{11} SiF_3 out-of-phase torsion (not obsd)
B_1 (R, ir)		1270 s, br			1206 s	1208	ν_{12} Si–O–Si antisym str (96%), SiF_3 sym def (4%)
		981 vs			989 m, sh	993	ν_{13} SiF_3 antisym str (92%), SiF_3 antisym def (6%), SiF_3 rock (2%)
		836 ms			838 ms	838	ν_{14} SiF_3 sym str (90%), SiF_3 sym def (10%)
		410 s			402 m	407	ν_{15} SiF_3 sym def (70%), SiF_3 sym str (21%), Si–O–Si antisym str (9%)
	341 w	343 vw, sh		(341 w)[c]		355	ν_{16} SiF_3 antisym def (85%), SiF_3 antisym str (15%)
	186 m		180 w (dp)	182 vw (dp)	179 m	167	ν_{17} SiF_3 rock (98%), SiF_3 antisym def (2%)
B_2 (R, ir)	934 ms	940 w, sh	942 ms	949 s		944	ν_{18} SiF_3 antisym str (91%), SiF_3 SiF_3 antisym def (7%), SiF_3 rock (2%)
				440 vw	434 ms	463	ν_{19} SiF_3 antisym def (90%), SiF_3 antisym str (6%), SiF_3 rock (4%)
	224 m	227 vw	221 m (dp)	225 mw (dp)		259	ν_{20} SiF_3 rock (81%), SiF_3 antisym def (19%)
							ν_{21} SiF_3 in-phase torsion (not obsd)

[a] Abbreviations used: v, very; s, strong; m, medium; w, weak; sh, shoulder; br, broad; p, polarized; dp, depolarized. [b] Refer to text. [c] Solid-phase frequency.

center. Other spectra taken immediately after attempting to purify the sample of $(F_3Si)_2O$ were even more revealing about this obscured fundamental. The infrared spectrum of the solid shows that this motion shifts to 410 cm^{-1} and is indeed relatively intense. The SiF_3 antisymmetric deformations (in phase) are assigned to the medium weak, polarized Raman line at 461 cm^{-1} for the A_1 fundamental and the medium strong infrared band at 434 cm^{-1} with corresponding Raman counterpart at 440 cm^{-1} for the B_2 motion. The out-of-phase antisymmetric deformations are observed at 358 and 341 cm^{-1} for the A_2 and B_1 motions, respectively. The later frequency was taken from the spectrum of the solid for the purpose of the normal-coordinate analysis because in the gas phase the line is believed to be obscured under the shoulder on the low-frequency side of the SiF_4 fundamental in that region. In the spectrum of the solid, the lines are better separated and consequently more distinct. The presence of a very weak infrared counterpart for this frequency at 343 cm^{-1} in the solid indicated it as the B_1 fundamental. An alternative choice for this assignment would be the weak infrared band at 309 cm^{-1}. However, this frequency is felt to be too low and is assigned instead as the overtone of a low-frequency SiF_3 rocking mode.

The lowest frequency modes of the SiF_3 groups are expected to be the rocking motions. The polarized Raman line at 242 cm^{-1} is attributed to the A_1 SiF_3 rock (in plane). The corresponding out-of-plane rock (B_2) is assigned to the Raman line at 225 cm^{-1}. The A_2 and B_1 rocks are found at 157 and 182 cm^{-1} in the Raman effect, the latter with an infrared counterpart at 179 cm^{-1}, hence, its assignment to the B_1 fundamental.

The Si–O–Si skeletal motions consist of an antisymmetric stretch, a symmetric stretch, and a bending motion. These modes are assigned at 1206 cm^{-1} in the infrared spectra, 598 cm^{-1} in the Raman spectra with an infrared counterpart at 601 cm^{-1}, and 85 cm^{-1} in the infrared spectra, respectively. Attempts to observe the Si–O–Si bend in the Raman effect were unsuccessful although this motion has been recently observed in the Raman spectrum of hexachlorodisiloxane.[10]

The SiF_3 torsions, ν_{11} and ν_{21}, were not observed in this study. For a reasonable guess of less than 2.00 kcal/mol for the SiF_3 torsional barrier, a calculation based on the harmonic approximation using structural parameters obtained from

Table II. Symmetry Coordinates Used in the Normal-Coordinate Analysis

Species (C_{2v})	Symmetry coordinates[a]	Description
A_1	$S_1 = r_{12} + r_{23}$	Si-O-Si sym str
	$S_2\ (2t_{14} - t_{15} - t_{16} + (2t_{37} - t_{38} - t_{39})$	SiF_3 antisym str (in phase)
	$S_3 = (t_{14} + t_{15} + t_{16}) + (t_{37} + t_{38} + t_{39})$	SiF_3 sym str (in phase)
	$S_4 = (\gamma_{415} + \gamma_{416} + \gamma_{516} - \beta_{214} - \beta_{215} - \beta_{216}) + (\gamma_{738} + \gamma_{739} + \gamma_{839} - \beta_{237} - \beta_{238} - \beta_{239})$	SiF_3 sym def (in phase)
	$S_5 = (2\gamma_{516} - \gamma_{415} - \gamma_{416}) + (2\gamma_{839} - \gamma_{738} - \gamma_{739})$	SiF_3 antisym def (in phase)
	$S_6 = (2\beta_{214} - \beta_{215} - \beta_{216}) + (2\beta_{237} - \beta_{238} - \beta_{239})$	SiF_3 in-plane rock (in phase)
	$S_7 = \alpha$	Si-O-Si bend
	$S_8 = (\gamma_{415} + \gamma_{416} + \gamma_{516} + \beta_{214} + \beta_{215} + \beta_{216}) + (\gamma_{738} + \gamma_{739} + \gamma_{839} + \beta_{237} + \beta_{238} + \beta_{239})$	Redundancy
A_2	$S_9 = (t_{15} - t_{16}) - (t_{38} - t_{39})$	SiF_3 antisym str (out of phase)
	$S_{10} = (\gamma_{415} - \gamma_{416}) - (\gamma_{738} - \gamma_{739})$	SiF_3 antisym def (out of phase)
	$S_{11} = (\beta_{215} - \beta_{216}) - (\beta_{238} - \beta_{239})$	SiF_3 out-of-plane rock (out of phase)
	$S_{12} = \tau_{3214} + \tau_{1237}$	SiF_3 torsion (out of phase)
B_1	$S_{13} = r_{12} - r_{23}$	Si-O-Si antisym str
	$S_{14} = (2t_{14} - t_{15} - t_{16}) - (2t_{37} - t_{38} - t_{39})$	SiF_3 antisym str (out of phase)
	$S_{15} = (t_{14} + t_{15} + t_{16}) - (t_{37} + t_{38} + t_{39})$	SiF_3 sym str (out of phase)
	$S_{16} = (\gamma_{415} + \gamma_{416} + \gamma_{516} - \beta_{214} - \beta_{215} - \beta_{216}) - (\gamma_{738} + \gamma_{739} + \gamma_{839} - \beta_{237} - \beta_{238} - \beta_{239})$	SiF_3 sym def (out of phase)
	$S_{17} = (2\gamma_{516} - \gamma_{415} - \gamma_{416}) - (2\gamma_{839} - \gamma_{738} - \gamma_{739})$	SiF_3 antisym def (out of phase)
	$S_{18} = (2\beta_{214} - \beta_{215} - \beta_{216}) - (2\beta_{237} - \beta_{238} - \beta_{229})$	SiF_3 in-plane rock (out of phase)
	$S_{19} = (\gamma_{415} + \gamma_{416} + \gamma_{516} + \beta_{214} + \beta_{215} + \beta_{216}) - (\gamma_{738} + \gamma_{739} + \gamma_{839} + \beta_{237} + \beta_{238} + \beta_{239})$	Redundancy
B_2	$S_{20} = (t_{15} - t_{16}) + (t_{38} - t_{39})$	SiF_3 antisym str (in phase)
	$S_{21} = (\gamma_{415} - \gamma_{416}) + (\gamma_{738} - \gamma_{739})$	SiF_3 antisym def (in phase)
	$S_{22} = (\beta_{215} - \beta_{216}) + (\beta_{238} - \beta_{239})$	SiF_3 out-of-plane rock (in phase)
	$S_{23} = \tau_{3214} - \tau_{1237}$	SiF_3 torsion (in phase)

[a] Not normalized; refer to Figure 4 for notation.

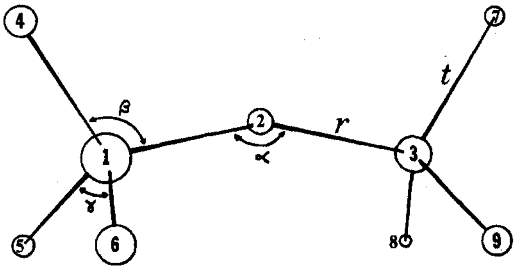

Figure 4. Hexafluorodisiloxane ($F_3SiOSiF_3$) with atoms and internal coordinates labeled.

electron diffraction data[8] indicates that the frequency of an SiF_3 torsion should be around 30 cm^{-1}. The in-phase and out-of-phase torsions of hexafluorodisiloxane would be expected to fall at higher and lower frequencies, respectively, than those given by the harmonic approximation with the magnitude of the shift determined by the degree of coupling of the two tops.[22]

Normal-Coordinate Analysis

No previous calculations have been reported for the force constants or normal coordinates of $F_3SiOSiF_3$. The assumed structure was taken from parameters determined by the electron diffraction technique:[8] Si–O distances, 1.580 Å; Si–F distances, 1.554 Å; Si–O–Si angle, 155.7°; F–Si–F angle, 108.8°. Twenty-three internal coordinates were defined as the basis set for the equations of motion and were used to construct the symmetry coordinates listed in Table II (refer to Figure 4). Nineteen valence force field constants were chosen including five principal and fourteen interaction constants. Schachtschneider's perturbation program[23] was used to adjust the force constants for a best fit to the observed frequencies and to test the constants for significance. Because of the importance of the J^tWJ matrix in the least-squares equation, the determinant of the matrix was tested after each iteration for singularity by comparing the product of the diagonal elements[24] to the determinant, and these two quantities were found to be of similar magnitude. The final constants which were found reproduced the observed frequencies to an average error of 10 cm^{-1} or 3%. The final force field is given in Table III from which the frequencies listed in Table I were calculated. The potential energy distribution, also given in Table I, shows that considerable mixing was observed among the symmetry coordinates, especially those in the A_1 block. Such extensive mixing is expected for this molecule because of the similar masses for fluorine and oxygen and the near-equality of the Si–F and Si–O force constants. The magnitude of the (Si–O)–(Si–F) interaction force constant illustrates these effects. The greatest mixing observed in the A_1 block involved the SiF_3 symmetric deformation and rock.

Table III. Internal Force Constants for $F_3SiOSiF_3$

Force constant[a]	Description	Value,[b] mdyn/A
K_r	Si–O str	5.48 ± 0.13
K_t	Si–F str	5.07 ± 0.08
H_α	Si–O–Si bend	0.55 ± 0.10
H_β	O–Si–F bend	0.46 ± 0.03
H_γ	F–Si–F bend	1.52 ± 0.05
H_τ	Torsion	*c*
F_{rt}	Si–O str–Si–F str	0.91 ± 0.17
$F_{\beta\gamma}$	O–Si–F bend–F–Si–F bend	−0.12 ± 0.05
$F_{r\beta}$	Si–O str–O–Si–F bend	0.24 ± 0.07
$F_{\alpha\beta}$	Si–O–Si bend–O–Si–F bend	−0.22 ± 0.08
$F_{r\alpha}$	Si–O str–Si–O–Si bend	−0.28 ± 0.14
$F_{\gamma\gamma}$	F–Si–F bend–F–Si–F bend	0.14 ± 0.05
$F_{\beta\beta}$	O–Si–F bend–O–Si–F bend	0.05 ± 0.03
$F_{tt'}$	Si–F str–Si–F str	−0.26 ± 0.05
$F_{\beta\beta'}$	O–Si–F bend–O–Si–F bend	0.12 ± 0.06
$F_{\gamma\gamma'}$	F–Si–F bend–F–Si–F bend	−0.23 ± 0.05
$F_{\beta\gamma'}$	O–Si–F bend–F–Si–F bend	−0.09 ± 0.05
$F_{t\gamma'}$	Si–F str–F–Si–F bend	−0.38 ± 0.07
$F_{t\beta'}$	Si–F str–O–Si–F bend	−0.32 ± 0.06
$F_{r\beta'}$	Si–O str–O–Si–F bend	0.37 ± 0.07

[a] Valence force field constants; prime indicates interaction between nonadjacent internal coordinates. [b] All bending coordinates weighted by 1 A. [c] Not calculated; fundamental not observed.

Table IV. Comparison of Force Constants, Skeletal Parameters, and Skeletal Frequencies in Some Disiloxanes

Molecule	Si–O dist, Å	Si–O–Si angle, deg	Si–O force const, mdyn/Å	Si–O–Si ν_{sym}, cm^{-1}	Si–O–Si ν_{anti} cm^{-1}
$H_3SiOSiH_3$	1.634[a]	144.1[a]	5.05[b]	606[c]	1107[c]
$(CH_3)_3SiOSi(CH_3)_3$	1.63[d]	130[d]	4.27[b]	520[e]	1060[e]
$Br_3SiOSiBr_3$			5.12[b]	685[b]	1094[b]
$Cl_3SiOSiCl_3$	1.592[f]	146[f]	5.38[b]	730[g]	1131[g]
$F_3SiOSiF_3$	1.580[h]	155.7[h]	5.48[i]	598[i]	1206[i]

[a] Reference 3. [b] Reference 21. [c] Reference 26. [d] Reference 27. [e] Reference 28. [f] Reference 9. [g] Reference 10. [h] Reference 8. [i] This work.

In addition to the 19 force constants listed in Table III, the interaction constants F_{tt}, $F_{t\gamma}$, F_{rr}, $F_{r\beta}$, $F_{r\alpha}$, $F_{r\gamma}$, $F_{\alpha\gamma}$, $F_{rt'}$, and $F_{r\gamma'}$ were calculated, but their values were all less than 0.03 mdyn/Å, and the frequency fit was not appreciably improved with the additional force constants. Therefore, these force constants were excluded from the final force field.

The Si–O stretching force constant reflects the increase in strength of the Si–O bond as the Si–O–Si angle opens compared to other substituted disiloxanes. In Table IV are compared the values of this force constant with the skeletal parameters and the frequencies of the symmetric and antisymmetric Si–O–Si stretches for several disiloxanes. In hexabromo- and hexachlorodisiloxane[21] the Si–O stretching force constants were calculated to be 5.12 and 5.38 mdyn/Å, respectively, compared to 5.48 mdyn/Å determined for hexafluorodisiloxane in this study. The Si–O–Si antisymmetric stretch occurs at 1107, 1131, and 1206 cm^{-1} for disiloxane and hexachloro- and hexafluorodisiloxane, respectively, in accord with the increase in strength of the Si–O bond in this series. The anomalously low frequency observed for the Si–O–Si symmetric stretching motion in hexafluorodisiloxane is explained by the significant coupling of this motion with the low-frequency SiF_3 symmetric deformation.

Discussion

The analysis of the infrared and Raman spectra of hexafluorodisiloxane has led us to the conclusion that the molecular symmetry of the molecule is C_{2v} in the gas, liquid, and solid states. This conclusion is in contrast to that in hexachlorodisiloxane whose Si–O–Si skeleton approaches linearity in the solid state and which was recently assigned under D_{3h} symmetry in this phase.[10] Apparently, the crystal packing factors that were advanced as an explanation of this behavior for the chlorinated compound are not operative to such an extent in hexafluorodisiloxane. It should be noted that rather large frequency shifts upon solidification in key fundamentals such as the A_1 SiF_3 symmetric stretch (−18 cm^{-1}), the Si–O–Si antisymmetric stretch (+64 cm^{-1}), and the Si–O–Si symmetric stretch (−19 cm^{-1}) were observed suggesting a small opening of the Si–O–Si angle in the solid phase. However, the spectra of this phase were not found to be markedly simplified by the disappearance of several low-frequency bands compared to the spectra of the gas as was the case with hexachlorodisiloxane.

Admittedly, the distinction between C_{2v} and C_2 symmetries is not a clear-cut one. Based on the polarization data from the Raman gas and liquid, particularly for the lower frequency motions, and the lack of infrared coincidences for the A_2 fundamentals we have chosen C_{2v} symmetry as that which best represents our data.

A sampling problem that arose in obtaining spectra for the solid phase involved the annealing procedure. In each case, the sample was carefully annealed even to the point of considerable loss of sample from the substrate. However, the spectra of the solid, particularly for the mid-infrared solid, did not exhibit the decrease in bandwidth and general clarity that are usually characteristic of spectra for this phase as compared to the spectra of the gas. It is felt that the presence of SiF_4 in the lattice of hexafluorodisiloxane prevented the redistribution to a uniform crystalline state upon annealing. At present, there seems to be no way of isolating the sample from SiF_4.[11] The Raman spectrum of the solid phase was handled by a different method than the infrared spectra and, consequently, did not exhibit these problems to any great extent. The behavior of the low-frequency fundamentals in the Raman effect was used to conclude that the molecular symmetry in the solid state did not change from that of the gas.

The results collected in Table IV suggest changes in bonding with substituent changes for the Si–O–Si skelton. As the electron-withdrawing potential of the substituents increases, the Si–O–Si angle and the Si–O force constant increase in a regular fashion. The opening of this angle reflects an increase in the amount of d_π–p_π bonding taking place between the silicons and oxygen. The delocalization of the oxygen lone pairs is expected to result in an increase in strength between the Si–O bonds and normal-coordinate calculations have verified this expectation.

Recently, an analysis of the Raman spectrum of liquid $Cl_3SiOSiF_3$[25] was presented. This publication was the first work reported on molecules of the type $X_3SiOSiY_3$. The molecular symmetry suggested for $Cl_3SiOSiF_3$ was C_{3v} or C_3 based on the relative simplicity of the spectrum. In order to better compare the vibrational and molecular symmetry results of this and other $X_3SiOSiY_3$ molecules to the results determined for $X_3SiOSiX_3$ molecules, the vibrational analysis should be extended to the gas phase and particularly to the solid phase for both the infrared and Raman effects. The spectra of the solid compared to those of the gas have been shown to provide information about both the molecular symmetry and changes in symmetry that may occur upon solidification.[10]

The vibrational analysis reported herein shows that hexafluorodisiloxane obeys C_{2v} selection rules in the gas phase and that this symmetry is maintained in going to the liquid and solid states. These findings are in contrast to those for hexachlorodisiloxane[10] which was recently shown to have C_{2v} symmetry in the gas phase but D_{3h} symmetry for the solid. The spectra presented here for $F_3SiOSiF_3$ do not exhibit the drastic changes in intensity for several bands upon condensation and the disappearance of a number of lower frequency lines in the Raman spectrum upon solidification as was observed for $Cl_3SiOSiCl_3$. Consistent trends among Si–O–Si skeletal parameters and frequencies have also been shown to exist. With these results the molecular structure and force constants of other substituted disiloxanes should be able to be predicted with some degree of certainty. Other investigators[29,30] have also discussed correlations among disiloxanes and have elaborated on the utility of vibrational spectroscopy in evaluating the structure and bonding in these molecules. The investigation of other disiloxanes, particularly those of the type $X_3SiOSiY_3$, will provide a test of the consistencies observed for the molecules already studied.

Acknowledgment. The authors thank Dr. F. E. Brinckman of the National Bureau of Standards for the preparation and donation of the sample. The authors also gratefully acknowledge the financial support of this study by the National Science Foundation through Grant GP-20723.

Registry No. $(F_3Si)_2O$, 14515-39-0.

References and Notes

(1) Part VII: J. R. Durig, W. O. George, Y. S. Li, and R. O. Carter, *J. Mol. Struct.*, **16**, 47 (1973).
(2) Taken in part from the thesis of M. J. Flanagan, to be submitted to the Department of Chemistry in partial fulfillment of the Ph.D. degree.
(3) A. Almenningen, O. Bastiansen, V. Ewing, K. Hedberg, and M.

Traetteberg, *Acta Chem. Scand.*, **17**, 2455 (1963).

(4) D. W. Robinson, W. J. Lafferty, J. R. Aronson, J. R. Durig, and R. C. Lord, *J. Chem. Phys.*, **35**, 2245 (1961).

(5) O. Bastiansen and M. Traetteberg, *Acta Crystallogr.*, **13**, 1108 (1960).

(6) Y. Morino, *Acta Crystallogr.*, **13**, 1107 (1960).

(7) U. Blukis, P. H. Kasai, and R. J. Myers, *J. Chem. Phys.*, **38**, 2753 (1963).

(8) W. Airey, C. Glidewell, D. W. Rankin, A. G. Robiette, G. M. Sheldrick, and D. W. Cruickshank, *Trans. Faraday Soc.*, **66**, 551 (1970).

(9) W. Airey, C. Glidewell, A. G. Robiette, and G. M. Sheldrick, *J. Mol. Struct.*, **8**, 413 (1971).

(10) J. R. Durig, M. J. Flanagan, and V. F. Kalasinsky, *J. Mol. Struct.*, **27**, 241 (1975).

(11) J. L. Margrave, K. G. Sharp, and P. W. Wilson, *J. Am. Chem. Soc.*, **92**, 1530 (1970).

(12) K. Hamada and H. Morishita, *Nagasaki Daigaku Kyoikugakubu Shizen Kagaku Kenkyu Hokoku*, **24**, 37 (1973).

(13) H. S. Booth and R. A. Osten, *J. Am. Chem. Soc.*, **67**, 1092 (1945).

(14) F. A. Miller and B. M. Harney, *Appl. Spectrosc.*, **24**, 291 (1970).

(15) R. N. Jones and A. Nadeau, *Spectrochim. Acta*, **20**, 1175 (1964).

(16) F. G. Baglin, S. F. Bush, and J. R. Durig, *J. Chem. Phys.*, **47**, 2104 (1967).

(17) R. T. Hall and J. M. Dowling, *J. Chem. Phys.*, **47**, 2459 (1967); **52**, 1161 (1970).

(18) R. J. H. Clark and D. M. Rippon, *J. Mol. Spectrosc.*, **44**, 479 (1972).

(19) E. A. Jones, J. S. Kirby-Smith, P. J. H. Woltz, and A. H. Nielsen, *J. Chem. Phys.*, **19**, 242 (1951); F. Bassette, A. Cabana, R. P. Fourier, and R. Savoie, *Can. J. Chem.*, **48**, 410 (1970).

(20) W. R. Thorson and I. Nakagawa, *J. Chem. Phys.*, **33**, 996 (1960).

(21) H. Bürger, K. Burczyk, F. Höfler, and W. Sawodny, *Spectrochim. Acta Part A*, **25**, 1891 (1969).

(22) J. R. Durig, S. M. Craven, and W. C. Harris in "Vibrational Spectra and Structure", Vol. I, J. R. Durig, Ed., Marcel Dekker, New York, N.Y., 1972, Chapter 4.

(23) J. H. Schachtschneider, "Vibrational Analysis of Polyatomic Molecules. Parts V and VI", Technical Reports No. 231-64 and 57-65, Shell Development Co., Emeryville, Calif., 1964 and 1965.

(24) J. Aldous and J. M. Mills, *Spectrochim. Acta*, **18**, 1073 (1962); **19**, 1567 (1963).

(25) K. Hamada, *J. Phys. Soc. Jpn.*, **36**, 617 (1974).

(26) R. C. Lord, D. W. Robinson, and W. C. Schumb, *J. Am. Chem. Soc.*, **78**, 1327 (1956).

(27) M. Yokoi, *Bull. Chem. Soc. Jpn.*, **30**, 100, 106 (1957).

(28) D. W. Scott, J. F. Messerly, S. S. Todd, G. B. Guthrie, I. A. Hossenlopp, R. T. Moore, A. Osborn, W. T. Berg, and J. P. McCullough, *J. Phys. Chem.*, **65**, 1320 (1961).

(29) R. J. Gillespie and E. A. Robinson, *Can. J. Chem.*, **42**, 2496 (1964).

(30) A. N. Lazarev, *Izv. Akad. Nauk SSSR, Ser. Khim.*, 235 (1964).

Contribution from the Department of Chemistry,
University of South Carolina, Columbia, South Carolina 29208

Microwave, Infrared and Raman Spectra, Structure, Dipole Moment, and Vibrational Assignment of Dimethylcyanosilane

J. R. DURIG,* P. J. COOPER,[1] and Y. S. LI

Received March 27, 1975 AIC502265

The microwave spectrum of dimethylcyanosilane has been investigated in the region between 18.0 and 40.0 GHz. Only A-type transitions were observed. The R-branch assignments have been made for the ground and three excited vibrational states. With reasonable assumptions made for the structural parameters of the dimethylsilyl moiety and the nitrile bond, the following structural parameters were obtained: $r(\mathrm{Si{-}CN}) = 1.840$ Å, $\angle(\mathrm{CSiC}) = 112.25°$, and an angle between the CSiC plane and the $\mathrm{Si{-}C{\equiv}N}$ bond of 123.97°. The dipole moment components were determined from the Stark effect to be $\mu_a = 3.65 \pm 0.1$ D and $\mu_c = 1.04 \pm 0.1$ D with a total dipole moment of 3.8 ± 0.1 D. The Raman spectra of dimethylcyanosilane have been studied to within 50 $\mathrm{cm^{-1}}$ of the exciting line in all three physical states. The infrared spectra of dimethylcyanosilane have been studied from 200 to 4000 $\mathrm{cm^{-1}}$ in the gaseous state and from 95 to 4000 $\mathrm{cm^{-1}}$ in the solid state. A vibrational assignment has been made, and from the low-frequency vibrational data, an upper limit of 2.8 kcal/mol was obtained for the barrier to internal rotation of the methyl groups.

Introduction

Recently, in this laboratory, microwave studies were completed on dimethylcyanamide, $(CH_3)_2NCN$,[2] dimethylcyanophosphine, $(CH_3)_2PCN$,[3] and isopropyl cyanide, $(CH_3)_2CHCN$[4] in order to determine the effects of the strong electron-withdrawing group CN on the molecular structure. In addition, there exists the possibility of bonding through the nitrogen of the CN group to form the isocyanide compound. A recent investigation of trimethylcyanosilane, $(CH_3)_3SiCN$, by Durig et al.[5] established the presence of an appreciable amount of the isocyanide at ambient temperature for this sample. As an extension of this work and as a continuation of our studies on the spectra and structure of silicon-containing compounds in general, a microwave investigation of dimethylcyanosilane has been undertaken.

The infrared and Raman spectra of the dimethylhalosilanes $(CH_3)_2SiHX$ (X = F, Cl, Br, I) have been analyzed in this laboratory,[6] and the torsional barrier heights for each compound reported. Therefore, in order to extend this series, infrared and Raman data were obtained for dimethylcyanosilane and a complete vibrational assignment is presented.

Experimental Section

The sample used in the present work was prepared by the following method. Samples of $(CH_3)_2SiHCl$ (12 g) and AgCN (6.7 g) were combined together with 70 ml of anhydrous diethyl ether in a round-bottomed flask which was attached to a high-vacuum system employing greaseless stopcocks. The mixture was then stirred at room temperature under an inert atmosphere for 36 hr. Materials volatile at −45° were allowed to distil from the reaction vessel for a period of 6 hr. Fractionation of the involatile materials yielded crude $(CH_3)_2SiHCN$ in a trap at −78°. Pure $(CH_3)_2SiHCN$ was obtained using a low-temperature sublimation column. The yield was 48% based on the initial amount of AgCN.

The rotational spectrum of dimethylcyanosilane was recorded in the frequency range 18.0–40.0 GHz using a Hewlett-Packard Model 8460A MRR spectrometer with 33.33-kHz square-wave Stark modulation. The Stark cell was maintained at Dry Ice temperature for all measurements except those of relative intensity, which were performed at room temperature. Sample pressure was held to about 20 μ. The accuracy in the line frequency measurement is estimated to be better than 0.2 MHz. The sample was observed to decompose in the wave guide even at Dry Ice temperature, requiring the sample to be renewed approximately every 20 min.

The Raman spectra were recorded with a Cary Model 82 Raman spectrometer equipped with a Spectra-Physics Model 171 argon ion laser. The 5145-Å line was used and the laser power was varied from 1 to 4 W at the head depending on the physical state under investigation. A standard Cary gas cell with the multipass optics was utilized to obtain the spectrum of gaseous dimethylcyanosilane, while a simple capillary tube was employed to obtain the spectrum of the liquid. The spectrum of solid $(CH_3)_2SiHCN$ was recorded by subliming the sample onto a standard cold cell maintained at liquid nitrogen temperatures.

The infrared spectra of dimethylcyanosilane between 200 and 4000 $\mathrm{cm^{-1}}$ were recorded with a Perkin-Elmer Model 621 spectrophotometer. A Beckman IR-11 spectrophotometer was used to record the infrared spectra between 33 and 300 $\mathrm{cm^{-1}}$. Both instruments were purged with dry air and calibrated with standard gases.[7] A 25-cm cell equipped with cesium iodide windows was used in recording the